行政院國家科學委員會專題研究計畫　成果報告

台灣西南部化石珊瑚礁的發育和衰退過程及其古海洋環境的研究(2/2)

計畫類別： 個別型計畫
計畫編號： NSC91-2611-M-002-022-
執行期間： 91 年 08 月 01 日至 92 年 07 月 31 日
執行單位： 國立臺灣大學海洋研究所

計畫主持人： 戴昌鳳

報告類型： 完整報告

處理方式： 本計畫可公開查詢

中　華　民　國 92 年 11 月 3 日

Cold seep carbonate hardgrounds for the initial development of scleractinian reefs in siliciclastic dominant environments.

SHIH-WEI WANG[1,2], SHOU-YEH GONG[1] and CHANG-FENG DAI[2*]

[1] Division of Geology, National Museum of Natural Science, No.1, Kuan Chien Road, Taichung 404, Taiwan

[2] Institute of Oceanography, National Taiwan University, No.1, Sec. 4, Roosevelt Road, Taipei 106, Taiwan

Running title: Cold seep carbonate hardgrounds for reef development

* Corresponding author. Institute of Oceanography, National Taiwan University,
P. O. Box 23-13, Taipei 106, Taiwan, R.O.C.
Fax: +886-2-23916693
e-mail: corallab@ccms.ntu.edu.tw

ABSTRACT

Pleistocene scleractinian reefs in SW Taiwan developed on several local structural highs that were closely associated with anticlines and faults in a Plio-Pleistocene foreland basin. Lithological successions of these fossil reefs are characterized by rapid facies changes from the underlying mudstone foundations upward into fossiliferous mudstones, then into reef limestone lithofacies. This study investigated how these coral reefs were able to establish in an environment dominated by fine-grained siliciclastics. Detailed studies of 3 quarry outcrops and 44 borehole cores reveal 5 types of local pioneering sedimentation at or near the base of the carbonates: (1) mound-like dolomitic mudstones, (2) dolomitic lithoclasts, (3) dolomitic conglomerates, (4) chimney-like dolomitic tubes, and (5) plume-like dolomitic mudstones. Abundant *in situ* lucinid bivalves were found from one of the mound-like dolomitic mudstones, with the tops encrusted with coralline algae, then overlaid by bioclastic limestone. In addition, four types of facies changes from underlying mudstone upward into the bottom of the reefal limestone were recognized. These successions suggest that the mudstone substrates at many locations were firm ground or hardground before the development of coral reefs, and served as the substrate on which sessile organisms were able to colonize in a muddy environment. According to the co-occurrences of dolomitic mudstones and fossil lucinids, as well as the tectonic setting of the study area, it is suggested that cold seep carbonates developed during shallowing of the structural highs in SW Taiwan, and served as the hardground and carbonate factories for the initial development of coral reefs in the siliciclastic environment. The occurrences of dolomitic lithoclasts, muddy conglomerate, and scouring of the upper most mudstones mark an erosional event occurred on these structural highs. It suggests that these lithologies were formed and deposited as the result of gas hydrate degassing, which was possibly triggered by the impulsion of tectonic activities such as earthquakes.

Keywords Cold seep carbonates, coral reef, foreland basin, lucinids, dolomites.

INTRODUCTION

Modern coral reefs generally develop in clear, warm, and well-lighted tropical shallow marine environments. Excessive terrigenous sediments and accompanying nutrients are usually considered the severe threat to coral reefs (Hallock & Schlager, 1986; Rogers, 1990; Birkeland, 1997). However, several studies have shown that coral reefs can survive or develop in turbid waters (Johnson & Risk, 1987; Roberts, 1987; Acevedo *et al.*, 1989; Tudhope & Scoffin, 1994). Many fossil records suggest that the development of coral reefs is compatible with terrigenous deposits (e.g., Weiss *et al.*, 1978; Hayward, 1982; Taberner & Bosence, 1985; Purser *et al.*, 1987; Braga *et al.*, 1990; Strasser *et al.*, 1992). Studies have also indicated that modern coral reefs can develop in muddy environments, such as fringing reefs on the Queensland Shelf of NE Australia (Hopley *et al.*, 1983; Johnson & Risk, 1987), SE Phuket in Thailand (Tudhope & Scoffin, 1994; Scoffin & Le Tissier, 1998), and off the western coast of Hammond Island in the Torres Strait (Woodroffe *et al.*, 2000). However, these reefs were not initially constructed on muddy substrates. Instead, they were initiated on various substrates including rocky bottom (Hopley *et al.*, 1983; Tudhope & Scoffin, 1994; Scoffin & Le Tissier, 1998; Woodroffe *et al.*, 2000), shoreline gravel and boulders (Johnson & Risk, 1987), muddy coral rubble banks (Hopley *et al.*, 1983), and coarse unconsolidated sediments (Hopley *et al.*, 1983). It seems that coral reefs develop in a variety of shallow marine environments if hardground or coarse-grained siliciclastic substrate is available.

Recently, a special mode of coral reef development in a noncarbonate environment was recognized from deep waters, and it was closely associated with hydrocarbon seeps (Hovland, 1990; Roberts, 1992; Hovland & Thomsen, 1997; Henriet *et al.*, 1998; Hovland *et al.*, 1998). Hovland (1990) proposed a model for carbonate reef formation mainly based on results from ecological studies at deep sea vent communities. Such reefs form at locations containing high concentrations of bacteria and other microorganisms suspended in the water column as a result of seeping fluids that provide some of the energy basis and carbon source. Precipitation of early diagenetic minerals may occur, then sediment grains and skeletal remains are cemented together to produce a firm and solid substratum. Eventually, the reef may grow extensively, depending on other environmental factors and the intensity of the seep. This model can be used to explain the paradoxical reef build-ups, both modern and fossil ones, found in various sedimentary environments. However, few verifications of this model from detailed studies have been provided (Henriet *et al.*, 1998; Hovland et al. 1998).

The Pleistocene scleractinian reefs in SW Taiwan developed on several local structural highs in a foreland basin (Gong *et al.*, 1996, 1998; Lacombe *et al.*, 1997, 1999). Stratigraphically, these reefs are characterized by rapid facies changes from underlying massive mudstones upward into fossiliferous mudstones, then into the basement of the reef limestones. The massive mudstone foundations are part of the upper Lower Gutingkeng Formation that consists of terrigenous fine-grained siliciclastics which were deposited in outer shelf to upper continental slope environments. The fossiliferous mudstones consist of terrigenous siliciclastics and bioclasts that are considered transitional lithofacies from the underlying siliciclastic mudstones upward into reefal limestones (Gong *et al*., 1998). The lowest strata of these coral reefs are mainly composed of bioclasts. Sharp contacts were observed at the Panpingshan and Hsiaokangshan quarries (Chen *et al*., 1994; Gong *et al*., 1998), where bioclastic limestones are deposited directly above a scoured surface into mudstones. Chen *et al*. (1994) suggested that there were some kind of sedimentological (erosional) events intervening between them. However, it is still uncertain how these Pleistocene coral reefs became established on muddy substrates. The aim of this study was to investigate the possible mechanisms that induced or led to the initial development of the Pleistocene coral reefs in SW Taiwan from a facies successional point of view.

MATERIALS AND METHODS

Field work was mainly carried out at quarry outcrops of NW and E Takangshan, as well as E Hsiaokangshan in SW Taiwan (Fig. 1). In addition, 44 borehole cores stored in the National Museum of Natural Science (NMNS) were studied, including 19 cores from the quarry of NW Takangshan (Fig. 2a), 18 cores from E Takangshan (Fig. 2b), and 7 cores from Panpingshan (Fig. 1c). Facies changes from underlying mudstones upward to the base of the reefal limestones were carefully examined. Principal mineralogical compositions of 202 rock samples were identified by X-ray diffraction. Typical rock samples of the massive mudstone and fossiliferous mudstone were selected from borehole core no. 9 of E Takangshan for wet sieve analysis. The grains of each sieved grade were identified using a binocular microscope, and particles were selected for X-ray diffraction analysis. The sand fraction of the fossiliferous mudstone was treated with diluted hydrochloric acid to remove the skeletal carbonates and then reweighed.

For comparison purposes, 3 outcrops in the Chiahsien area (Fig. 1d) were included in this study to improve our interpretation of the initiation of the dolomitic hardground and related sedimentations. These outcrops belong to the Pliocene Yenshuikeng Formation that was deposited in inner to outer shelf environments (Yeh & Chang, 1991). Lithologies of these outcrops are dominated by massive mudstones and thin-bedded sandstones. Many localized marl-like carbonate rocks, described as dolomitic mudstones and exposed at various localities within this formation, were examined in detail.

LITHOLOGIES

Exposed strata of the massive mudstones were usually less than 3 m thick at the quarry outcrops. An exception occurred at eastern Hsiaokangshan quarry, where the exposed mudstones were more than 50 m thick (Fig. 3c). This lithology consists of terrigenous clay and silt, containing abundant planktonic and benthic foraminifera, a few granule-sized pieces of woody detritus, and rare megafossils. Grain size analysis of a typical sample shows that approximately 98% weight fraction of the mudstone is composed of clay and silt, and the rest is composed of sand and granule-sized grains. The sand grains consist of planktonic and benthic foraminifera, bivalve fragments, woody detritus, quartz grains, lithic grains, pyrite grains and aggregates, and minute mica flakes, while the granule-grade particles are composed of pyrite aggregates. In addition, it is notable that the pyrite grains and aggregates together constitute more than 17.6% weight fraction of the sand grains.

Most of the mudstones are monotonous and without discernible bedding features. However, there are some subangular to subrounded dolomitic lithoclasts within the uppermost mudstones of the E Takangshan (Fig. 4e) and E Hsiaokangshan quarry outcrops. Similar lithoclasts were found within the upper 3 m strata of the mudstone facies in 6, 5, and 2 borehole cores (Fig. 4f) from NW Takangshan, E Takangshan, and Panpingshan quarries, respectively.

Four lithologies were identified in the transition zone from the underlying mudstones up into the reefal limestones: (1) dolomitic mudstones, (2) muddy conglomerates, (3) fossiliferous mudstones, and (4) bioclastic limestones.

(1) Dolomitic mudstones

Dolomitic mudstones are fine-grained mudstones cemented by dolomitic carbonates. This facies develops at the top of the mudstones, and is in turn overlain by bioclastic limestones. It may occur as mound-like lithological lenses, lithoclasts, chimney-like structures, or plume-like rock. However, only dolomitic lithoclasts were found in the borehole cores.

The results of X-ray diffraction analyses showed that the compositions of the dolomitic carbonates are diverse, including dolomite ($CaMg(CO_3)_2$), ferroan dolomite ($Ca(Mg,Fe)(CO_3)_2$), ankerite ($Ca(Mn,Mg,Fe)(CO_3)_2$), and kutnahorite ($Ca(Fe,Mg,Mn)(CO_3)_2$). A few of the dolomitic mudstones also contain calcite and/or aragonite minerals.

(1a) Mound-like dolomitic mudstones

Two well-lithified massive dolomitic mudstones outcrop at the quarries of E Takangshan (TKS-1 and TKS-2) (Fig. 2b) with limited lateral extensions and an outline of a mud-mound. TKS-1 is located about 100 m south of the outcrop of muddy conglomerates, where the uppermost 1 m strata of the dolomitic mudstones are exposed with a lateral extension of about 7 m. It contains many well-preserved fossil bivalves of *Loripes goliath* Yokoyama (Fig. 5e). Both the occurrences of the lithology and associated lucinid fossils are identical to those of Paiyunhsiangku at Chiahsien (Fig. 5a). However, the mineralogy of fossil shells at these 2 localities differed; the former was aragonite while the latter was sparry calcite. In addition, the topmost rocks of the dolomitic mudstone at TKS-1 were encrusted with laminated coralline algae of about 20 cm thick, then were overlain by bioclastic limestone (Fig. 3e). This indicates that the dolomitic mudstone at TKS-1 acted as the hardground for colonization of sessile organisms.

At TKS-2, the mound-like dolomitic mudstone is located near the outcrop of muddy conglomerates with a lateral extension of about 4.5 m. The occurrences of dolomitic mudstone at this locality are similar to those of TKS-1, but were overlain directly by bioclastic limestone with an erosional contact (Fig. 3f). In addition, there were far fewer fossil lucinids within the dolomitic mudstone at TKS-2 than at TKS-1.

At the Hsiaokangshan quarry, a similar lithology was found at the top of the massive mudstones with a lateral extension of more than 2 m. One specimen of an articulated fossil lucinid was collected from the rockwastes nearby. Both the carbonate minerals of this lithified mudstone and fossil shells were calcite, and differed from those of TKS-1 and TKS-2. Although the exposed mudstone strata at this quarry were very thick (> 50 m), the calcareous mudstone and fossil lucinids were found at the top of the mudstone lithofacies only.

(1b) Dolomitic lithoclasts

Dolomitic lithoclasts were found in 13 borehole cores, including 6 cores at NW Takangshan, 5 cores at E Takangshan, and 2 cores at Panpingshan (Figs 1c, 2a and b). The clasts occurred within a variety of lithologies, including massive mudstones, muddy conglomerates, fossiliferous mudstones, and bioclastic limestones.

In borehole cores and at the newly exposed outcrops, both the dolomitic lithoclasts and hosted mudstone are dark gray in color. The most reliable criteria to recognize them at fields are their hardness and resistance to weathering. Sizes of these well-lithified lithoclasts ranged from pebbles to cobbles, and were deposited as matrix-supported sedimentary fabrics in the mudstones.

At the eastern Hsiaokangshan quarry and in core no. 4 from Panpingshan, the dolomitic lithoclasts occurred only at the top horizons of the mudstone facies. In borehole core H-1 from E Takangshan, they occurred only at the top horizon of fossiliferous mudstone facies, while at the E Takangshan quarry and within another 11 cores, the dolomitic lithoclasts occurred sporadically within the uppermost 3 m strata of the mudstones (Fig. 4f). Of these, in borehole core no. 3 from E Takangshan, the dolomitic lithoclasts also occurred within the fossiliferous mudstone lithofacies. Based on these observations, the majority of dolomitic lithoclasts recognized from borehole cores were deposited within the massive mudstone lithofacies.

The dolomitic lithoclasts also occurred as coarse-grained constituents of muddy conglomerate at the E Takangshan quarry (Fig. 4c). The highest stratigraphic horizon of dolomitic lithoclast deposition is the bioclastic limestone at Panpingshan quarry where the clast served as the core for rhodolith growth.

(1c) Chimney-like structures

Many chimney-like structures ranging from 3 to 30 cm in diameter and protruding from the weathered mudstones were found at the quarries of E Takangshan and E Hsiaokangshan (Fig. 4a and b). The cross sections of these tubes were elliptical or nearly circular. Most tubes possessed a hollow center indicating that there was a conduit running through it. The orientation of most of these tubular structures was vertical, while some were slightly tilted. They occurred within the uppermost several meters of the mudstone facies.

In the Chiahsien area, many chimney-like structures occurred at the outcrops of Niupu (Fig. 5f) and Ssutehsiang. The center of most of these tubular structures was filled with sparry calcite. No encrusting organisms were found on the outer walls of the chimney-like tubes in this area.

(1d) Plume-like dolomitic mudstones

This lithology pierced through the muddy siltstones of the Pliocene Yenshuikeng Formation, and occurred at Ssutehsiang (Fig. 5b), where abundant large fossil bivalves of *L. goliath* were collected. The majority of fossil lucinids were collected from this dolomitic mudstone and the surrounding muddy siltstones. Evidence showed that all the fossil lucinids within the dolomitic mudstone were deposited *in situ* and were well-preserved (Fig. 5c), while those collected from the surrounding mudstones showed some degree of deformation (Fig. 5d). This suggests that syndepositional diagenesis occurred during the deposition of the dolomitic mudstones.

One mini plume-like dolomitic mudstone co-occurring with chimney-like structures was found at the eastern Hsiaokangshan quarry (Fig. 4d). The outer wall of this mini plume is ragged with a maximum diameter of 34 cm. Neither conduits nor fossil lucinids were found within this dolomitic mudstone.

(2) Muddy conglomerates

Muddy conglomerate lithofacies outcropped at the E Takangshan quarry (Fig. 4c) with a lateral extension of about 12 m. The thickness of this conglomerate is about 30 cm. Both the top and bottom of this lithology are bounded by scourings. This facies was deposited at the top of the massive mudstones, and was in turn overlain by bioclastic limestones. The underlying mudstones contain some dolomitic lithoclasts, and show the sedimentary fabric of matrix supporting.

This poorly sorted lithology consists of fine-grained siliciclastic matrix and dolomitic lithoclasts, and shows a matrix- to clast-supported sedimentary fabric. The shape and size of the lithoclasts within the muddy conglomerates are similar to those of the mudstone facies, indicating that both were likely derived from the same origin and/or had been deposited by the same mechanism. The lateral tracing of this lithofacies is impossible due to the limited outcrop. However, dolomitic lithoclasts repeatedly occurred in some borehole cores (e.g., N-8 at NW Takangshan, no. 2 at E Takangshan) (Fig. 4f), suggesting that this lithology may have been deposited on a broader scale on the topographic highs.

(3) Fossiliferous mudstones

This lithology is composed of poorly sorted dark gray mudstone with locally faint bedding (Fig. 3b). It varies in thickness from tens of centimeters to more than 13 m. Bioclasts within this lithology are much more diverse than those of the underlying massive mudstones, including planktonic, small and large benthic foraminifera, spicules of sponges and gorgonian corals, mushroom corals, foliaceous corals, dendroid and massive colonial corals, bryozoans, small articulated brachiopods, bivalves, gastropods, lime tubes of annelids, ostracods, chelipeds of crab, spines of sea urchins, otoliths of fish, rhodoliths, encrusting coralline algae, and carbonized woody detritus. Some rounded dolomitic and terrigenous metamorphic lithic grains were identified from the sieved sand-grade grains. Pyrite grains and aggregates are also present within the sand-grade particles but there are far fewer here than in the massive mudstones. Based on the results of grain size analysis, clay and silt grains constitute about 60.7% weight fraction of this lithology, sand grains account for about 38.2%, and the rest is composed of granular bioclastic grains. Of which, skeletal carbonates of sieved sands constitute 33.7% of the weight fraction of this lithology. Acid-insoluble resides of sieved sand grains constitute only a minute weight fraction (ca. 4.5%), and are composed of angular quartz grains, minute pyrite particles, and few rounded terrigenous lithic grains.

According to the occurrences of macrofossils, the majority of bioclasts within this lithology were abraded or stained with colors, and only a few complete mushroom corals and clypeiform urchins were found. Furthermore, the lower contact of this lithology was scouring, suggesting that those bioclasts were redeposited from nearby sources.

(4) Bioclastic limestones

This lithology constitutes the basal parts of the reefal limestones (Fig. 3d), and grade upward into reefal limestones. It mainly consists of rhodoliths and large foraminifera. The former is composed of coralline algae *Lithophyllum*, *Mesophyllum*, and the encrusting foraminifera *Acervulina*. The major large foraminifera are *Amphistegina*, *Heterostegina*, and *Baculogypsinoides*. Other types of bioclasts include smaller benthic foraminifera, dendroid and massive scleractinian corals, mushroom corals, bivalves, gastropods, spines of sea urchins, and geniculated coralline algae.

FACIES CHANGES

The lithologies described above may occur in different sequences, and there is no uniform sequence in the transition. The underlying mudstones may be overlain by fossiliferous mudstones, bioclastic limestones, dolomitic mudstones, or muddy conglomerates. Four types of facies associations were recognized from the transitions (Fig. 6).

1. Mudstone-fossiliferous mudstone-bioclastic limestone (Fig. 3a and b): In this facies association, the fossiliferous mudstone lithofacies is always overlain by bioclastic limestone. Both the top and bottom of the fossiliferous mudstone are bounded by scouring. At the NW Takangshan quarry, tubular ichnofossils that had burrowed into the mudstone were truncated at the upper facies contact and infilled with bioclasts. This suggests the firm-ground nature of the topmost mudstones. This type of facies change was observed at the NW Takangshan quarry outcrop and in most of the borehole cores, including 18 cores at NW Takangshan, 18 cores at E Takangshan, and 4 cores at Panpingshan. Of these, the dolomitic lithoclasts that occurred in the mudstone and/or fossiliferous mudstone were recognized from 12 cores.

2. Mudstone-bioclastic limestone (Fig. 3c and d): Facies change of this type is sharp, with the fossiliferous mudstone lithofacies missing. No loading structure was observed among them. The ichnofossils that had burrowed into the mudstone were truncated at the upper facies contact by scouring, and infilled with granule- to pebble-sized limestone lithic grains. These also suggest the firm-ground nature of the topmost mudstones. This type of facies association was observed at the E Hsiaokangshan quarry outcrop and in 4 borehole cores, including 1 core at NW Takangshan (core N-10), and 3 cores at Panpingshan (cores no. 4, B-7, B-8). Some dolomitic lithoclasts were observed at the top horizon of the mudstone lithofacies from the E Hsiaokangshan quarry outcrop and core no. 4 of Panpingshan.

3. Mudstone-dolomitic mudstone-bioclastic limestone (Fig. 3e and f): The dolomitic mudstone facies occurred as mound-like dolomitic mudstones at E Takangshan (TKS-1 and TKS-2) and probably in the E Hsiaokangshan quarries. The bottoms of both of these 2 dolomitic mudstones were unexposed. At TKS-1, the top of the mound-like dolomitic mudstone was encrusted with coralline algae. The top and bottom of the laminated corallines were both bounded by erosional surfaces. At TKS-2, the mound-like dolomitic mudstone was directly overlaid by bioclastic limestone with scouring.

4. Mudstone-muddy conglomerate-bioclastic limestone (Fig. 4c): This facies association only observed at the E Takangshan quarry outcrop. Both the top and bottom of the muddy conglomerate are bounded by scouring. Although the muddy conglomerate lithofacies probably occurred in the borehole cores N-8 at NW Takangshan and no. 2 at E Takangshan quarries, they were directly overlaid by fossiliferous mudstone. It appears that the lateral extension of this facies association is very limited.

Two mudstone outcrops that contain many chimney-like dolomitic pipes cannot be classified properly into any one of the facies associations mentioned above. In the E Takangshan quarry, the mudstone that was pierced by chimney-like dolomitic pipes outcropped among TKS-1 and TKS-2 (Fig. 2b, 4a). Where, more than 28 dolomitic pipes were observed within an area of 9 x 13 m^2. In the E Hsiaokangshan quarry, a similar mudstone is located near the outcrop of the mudstone- bioclastic limestone facies association (Fig. 3c, 4b). More than 37 dolomitic pipes and one mini plume-like dolomitic mudstone (Fig. 4d) were observed within an area of 21 x 27.5 m^2. It is notable that no chimney-like structure was found except in the mudstone lithofacies.

DISCUSSION

Dolomitic mudstones and fossil lucinids

This study shows that the initial development of coral reefs in SW Taiwan, indicated by transitions from siliciclastic mudstones to coral reefs, was associated with dolomitic mudstones. Various occurrences of dolomitic mudstones were found in the study area, including mound-like lithological lenses, lithoclasts, chimney- and plume-like rocks. Among them, the dolomitic lithoclasts were redeposited sedimentations, while the others were formed *in situ*. Several common features could be recognized from these *in situ* dolomitic mudstones.

1. They were developed in deeper and low-energy sedimentary environments.

2. They pierced through the muddy strata and weathered as positive features at outcrops. The freshly exposed dolomitic mudstones were dark gray, while those of weathered parts were buff to light tan in color. An odor of fire stink was emitted as the rock samples were collected, suggesting the anoxic depositional nature of the sedimentation.

3. The benthic macrofauna of the dolomitic mudstones was dominated by the fossil lucinid, *Loripes goliath*.

4. The fossil lucinids within the dolomitic mudstone were well preserved, while those in the surrounding mudstones were usually crushed or flattened. This indicates that the development of the dolomitic mudstone was accompanied by submarine cementation.

The fossil macrofaunas of both the mound-like and plume-like dolomitic mudstones were characterized by (1) a high density of bivalves, (2) a low species richness dominated by *L. goliath*; (3) the lucinid population mainly being composed of large individuals, mostly larger than 10 cm in shell length, and (4) very high articulation frequencies. These are typical features of ancient autochthonous and seep assemblages (Callender & Powell, 1992).

The extant species of the Lucinidae are burrow-dwelling bivalves that occur globally over a wide range of marine habitats from intertidal to deep-sea (Fisher, 1990; Anderson, 1995). Many lucinids burrow deeply and live near the interface of aerobic and anaerobic zones, or within the latter (Taylor & Glover, 2000). All species of the Lucinidae possess sulfide-oxidizing, chemosymbiotic bacteria housed in bacteriocytes of their gill filaments (Fisher & Hand, 1984; Giere, 1985; Reid & Brand, 1986; Distel & Felbeck, 1987; Frenkiel *et al.*, 1996; Taylor & Glover, 2000). Chemosymbiosis was suggested to be an inherent character of this family that can be traced to the Silurian lucinid *Ilionia* (Liljedahl, 1992; Taylor & Glover, 2000).

The co-occurrence of fossil lucinids and dolomitic mudstones in the study area indicates some special geological events. They are likely analogs of the Jurassic ‘pseudobioherm’ in SE France (Gaillard *et al*., 1992), Cretaceous ‘seep-related limestone mounds’ of NE Greenland (Kelly *et al.*, 2000), ‘Tepee Buttes’ in the Cretaceous Pierre Shale Formation of Colorado (USA) (Kauffman *et al.*, 1996), and the Miocene ‘calcari a *Lucina*’ (limestones with *Lucina* sp.) in the Italian north Apennines (Terzi, 1993). These are fossil analogs of recent methane-based cold seep complexes that occur at sites of concentrated pore-water expulsion in a variety of geological settings (Goedert & Squires, 1990; Campbell, 1992; Gaillard *et al*., 1992; Kauffman *et al*., 1996). The cold seep carbonates were suggested to have precipitated following syntrophic interactions of methane oxidizers and sulphate reducers, which were processed by a unique microbial consortium (Ritger *et al.*, 1987; Kulm & Suess, 1990; Beauchamp & Savard, 1992; Paull *et al.*, 1992; Peckmann *et al.*, 1999; Aharon, 2000; Boetius *et al.*, 2000; DeLong, 2000). These carbonates were precipitated below the oxic zone of sediments, probably no deeper than several centimeters to a few meters below the seabed (Ritger *et al.*, 1987), and they are characterized by abundant chemosynthetic bivalves, especially lucinids (Gaillard *et al*., 1992; Campbell & Bottjer, 1993).

The mound-like and plume-like dolomitic mudstones were possibly formed in areas where the fluid flow concentrated to form discrete venting (Campbell & Bottjer, 1993). The co-occurrence of lucinids with cold seep carbonates suggests that these ventings may have persisted for a period of time. The compactness of the cold seep carbonates indicates continuous active seepage rather than the sporadic expulsion of gas (Kelly *et al.*, 2000). The chimney-like structures that outcrop at E Takangshan, E Hsiaokangshan, and Niupu, Ssutehsiang in Chiahsien are likely fossil analogs of modern carbonate chimneys that represent discrete methane-related fluid venting (Kulm & Suess, 1990; Jensen *et al.*, 1992; Sakai *et al.*, 1992; Campbell & Bottjer, 1993; Lewis & Marshall, 1996). The wide occurrences of cold seep carbonates in the study area indicate that methane seeps developed extensively on the structural highs in SW Taiwan and possibly facilitated the initial development of coral reefs.

Facies changes and geological implications

The major facies change from the underlying mudstone to reef limestone is the ‘mudstone-fossiliferous mudstone-bioclastic limestone’. The fossiliferous mudstone represents the transition from siliciclastic to carbonate environments. However, there is no evidence of synsedimentary substrate modification by marine benthos in this type of transition. In addition, the majority of bioclasts in this lithology are fragmentary, and only a few complete macrofossils have been observed. It seems that the quantity of bioclasts suddenly increased and the bioclasts within the fossiliferous mudstone are allochthonous. This is further supported by the bottom scouring of this lithology. It is speculated that some kind of ‘carbonate factory’ existed on the structural highs and distributed bioclasts to the surrounding muddy environments, which eventually led to facies conversion. The mound-like cold seep dolomitic hardground which occurs at the E Takangshan quarry is likely an example of this. Since the lucinids associated with cold seep carbonates were deposited below the oxic zone of sediment (Ritger *et al.*, 1987), there were likely some erosional events occurred at or near the end of the mudstones deposition that scraped off the overlying soft sediments and uncovered the local hardgrounds. Elevation of the sites by thrust activity and possibly earthquakes associated with the thrusting might have provided conditions favorable for submarine scouring (Gong *et al*., 1998).

At the E Takangshan quarry, dolomitic lithoclasts occurred as ‘isolated load balls’ or ‘pseudonodules’ (Collinson & Thompson, 1989) suspended in the mudstone (Fig. 4e), suggesting that they were deposited as a result of bed loading. The associations of fossil lucinids and mound-like cold seep carbonates which occur nearby also suggest that the surrounding muddy substratum of that period was unconsolidated. However, no load deformation structure was observed in the overlying muddy dolomitic conglomerate. We speculate that these dolomitic lithoclasts were formed and deposited through some unusual mechanisms or events.

The co-occurrences of cold seep carbonates were documented in nearly all gas hydrate sites (Bohrmann *et al.*, 1998). The formation of cold seep carbonates is a strong indication of hydrate-related tectonic dewatering at active margin (Suess *et al.*, 1999). In addition, the degassing of gas hydrates may cause deep-sea slope failure, which is triggered by an increase in bottom-water temperatures (Kennett *et al.*, 2000) and/or the lessening of hydrostatic pressure through relative sea-level falling (Paull *et al.*, 1996; Maslin *et al.*, 1998). The expulsion of warmer fluids toward the sediment surface by tectonic impulsive activity (Suess *et al.*, 1999) and the tectonic uplift of gas hydrate sediment (McDonnell *et al.*, 2000) could also cause successive episodes of fluid-associated degassing. Recent studies confirm that gas hydrates of significant sizes occur within the offshore sediment depocenter adjacent to Taiwan (Chi *et al.*, 1998; McDonnell *et al.*, 2000), which is situated at the southwestward extension of the Plio-Pleistocene foreland basin. Destabilization of gas hydrates is possibly the mechanism that led to the top scouring of the mudstone facies.

Many researchers have proposed that gas violently escaping through surface sediments might lead to the formation of pockmarks, craters, and brecciated limestones (Hovland *et al.*, 1987; Hovland & Judd, 1988; MacDonald *et al*., 1990; Kauffman *et al.*, 1996; Reilly *et al.*, 1996). The occurrences of dolomitic lithoclasts in massive mudstones and muddy conglomerates suggest that similar events may have occurred in the study area. The widespread distributions of dolomitic lithoclasts further suggest that the episodic fluid explosions occurred extensively at the study sites, which is possibly linked to the impulsion of tectonic activities such as earthquakes. On a larger scale, the occurrences of dolomitic lithoclasts and scouring indicate the initiation of Pleistocene reef development on local structural highs in SW Taiwan. It appears that the initial foundations for reef development in SW Taiwan were more complicated than those suggested by the seepage-associated reef formation model (Hovland, 1990).

Reef formation is often dependent on the topography of the seabed (Longman, 1981). Topographic highs favor colonization and growth of reef builders, especially if the substrate is hardground or composed of coarse bioclasts (Birkeland, 1997). We propose that during the shallowing of topographic highs in SW Taiwan, the cold seep carbonates served as localized hardgrounds and acted as ‘carbonate factories’ for the surrounding environments that eventually led to the facies shifting in the sedimentary environment.

CONCLUSIONS

1. The development of coral reefs on mud foundations was promoted by a series of geological events, including the formation of structural highs, precipitation of cold seep carbonates, the occurrences of erosional events related to gas hydrate degassing, and the uncovering of hardgrounds and firmed grounds during shallowing of these topographic highs. Of which, the mound-like cold seep carbonates acted as the hardgrounds and carbonate factories for the initial development of coral reefs in the siliciclastic environment.

2. This is the first recognition of cold seep carbonates in the Taiwan region. They may occur extensively within the foreland basin of SW Taiwan, and may provide valuable information for reconstruction of the local tectonic history in the future.

ACKNOWLEDGEMENTS

This study was supported by the National Museum of Natural Science, and grants from the National Science Council of the Republic of China (NSC90-2611-M-002-006 and NSC91-2611-M-002-022).

REFERENCES

Acevedo, R., Morelock, J. and **Olivieri, R.A.** (1989) Modification of coral reef zonation by terrigenous sediment stress. *Palaios*, **4**, 92-100.

Aharon, P. (2000) Microbial processes and products fueled by hydrocarbons at submarine seeps. In: *Microbial sediments* (Eds R. E. Riding and S. M. Awramik), pp. 270-281. Springer-Verlag, New York.

Anderson, A.E. (1995) Metabolic responses to sulfur in lucinid bivalves. *Am. Zool*., **35**, 121-131.

Beauchamp, B. and **Savard, M.** (1992) Cretaceous chemosynthetic carbonate mounds in the Canadian Arctic. *Palaios*, **7**, 434-450.

Birkeland, C. (Ed.) (1997) *Life and death of coral reefs*. Chapman and Hall, New York, 536 pp.

Boetius, A., Ravenschlag, K., Schubert, C.J., Rickert, D., Widdel, F., Gieseke, A., Amann, R., Jorgensen, B.B., Witte, U. and **Pfannkuche, O.** (2000) A marine microbial consortium apparently mediating anaerobic oxidation of methane. *Nature*, **407**, 623-626.

Bohrmann, G., Greinert, J., Suess, E. and **Torres, M.** (1998) Authigenic carbonates from the Cascadia subduction zone and their relation to gas hydrate stability. *Geology*, **26**, 647-650.

Braga, J.C., Martin, J.M. and **Alcala, B.** (1990) Coral reefs in coarse-terrigenous sedimentary environments (upper Tortonian, Granada Basin, southern Spain). *Sed. Geol.*, **66**, 133-150.

Callender, W.R. and **Powell, E.N.** (1992) Taphonomic signature of petroleum seep assemblages on the Louisiana upper continental slope: recognition of autochthonous shell beds in the fossil record. *Palaios*, **7**, 388-408.

Campbell, K.A. (1992) Recognition of a Mio-Pliocene cold seep setting from the northwest Pacific convergent margin, Washington, U.S.A.. *Palaios*, **7**, 422-433.

Campbell, K.A. and **Bottjer, D.J.** (1993) Fossil cold seeps (Jurassic-Pliocene) along the convergent margin of western North America. *Natl. Geogr. Res. Explor*., **9**, 326-343.

Chen, H.W., Wu, L.C. and **Tsien, H.H.** (1994) Comformable contact relationships between the early Pleistocene limestones of Panpingshan and the Gutingken Formation in the Kaohsiung area, southern Taiwan. *Centr. Geol. Surv. Spec. Publ.*, **8**, 101-119. (in Chinese, with English abstract)

Chi, W.-C., Reed, D.L., Liu, C.-S. and **Lundberg, N.** (1998) Distribution of the bottom-simulating reflector in the offshore Taiwan collision zone. *TAO*, **9**, 779-794.

Chinese Petroleum Corporation (CPC) (1989) *Geological map of Tainan*, scale 1:100000, Chinese Soc. Survey Engineering, Taiwan.

Collinson, J.D. and **Thompson, D.B.** (1989) *Sedimentary structures*, 2nd Ed., Chapman and Hall, New York, 207 pp.

DeLong, E.F. (2000) Resolving a methane mystery. *Nature*, **407**, 577-578.

Distel, D.L. and **Felbeck, H.** (1987) Endosymbiosis in the lucinid clams, *Lucinoma aequizonata*, *Lucinoma annulata* and *Lucina floridana*: a reexamination of the functional morphology of the gills as bacteria-bearing organs. *Mar. Biol.*, **96**, 79-86.

Fisher, C.R. (1990) Chemoautotrophic and methanotrophic symbioses in marine invertebrates. *Rev. Aquat. Sci.*, **2**, 399-436.

Fisher, C.R. and **Hand, S.C.** (1984) Chemoautotrophic symbionts in the bivalve *Lucina floridana* from seagrass beds. *Biol. Bull.*, **167**, 445-459.

Frenkiel, L., Gros, O. and **Moueza, M.** (1996) Gill structure in *Lucina pectinata* (Bivalvia: Lucinidae) with reference to hemoglobin in bivalves with symbiotic sulphur-oxidizing bacteria. *Mar. Biol.*, **125**, 511-524.

Gaillard, C., Rio, M., Rolin, Y. and **Roux, M.** (1992) Fossil chemosynthetic communities related to vents or seeps in sedimentary basins: the pseudobioherms of southeastern France compared to other world examples. *Palaios*, **7**, 451-465.

Giere, O. (1985) Structure and position of bacterial endosymbionts in the gill filaments of Lucinidae from Bermuda (Mollusca, Bivalvia). *Zoomorphology*, **105**, 296-301.

Goedert, J.L. and **Squires, R.L.** (1990) Eocene deep-sea communities in localized limestones formed by subduction-related methane seeps, southwestern Washington. *Geology*, **18**, 1182-1185.

Gong, S.Y., Lee, T.Y., Wu, J.C., Wang, S.W. and **Yang, K.M.** (1996) Possible links between the development of Plio-Pleistocene coral reef limestones and thrust migration in southwestern Taiwan. *J. Geol. Soc. China*, **39**, 151-166.

Gong, S.Y., Wang, S.W. and **Lee, T.Y.** (1998) Pleistocene coral reefs associated with claystones, southwestern Taiwan. *Coral Reefs*, **17**, 215-222.

Hallock, P. and **Schlager, W.** (1986) Nutrient excess and the demise of coral reefs and carbonate platforms. *Palaios*, **1**, 389-398.

Hayward, A.B. (1982) Coral reefs in a clastic sedimentary environment: fossil (Miocene, S.W. Turkey) and modern (Recent, Red Sea) analogues. *Coral Reefs*, **1**, 109-114.

Henriet, J.P., De Mol, B., Pillen, S., Vanneste, M., Van Rooij, D., Versteeg, W., Croker, P.F., Shannon, P.M., Unnithan, V., Bouriak, S., Chachkine, P. and **The Porcupine-Belgica 97 Shipboard Party** (1998) Gas hydrate crystals may help build reefs. *Nature*, **391**, 648-649.

Hopley, D., Slocombe, A.M., Muir, F. and **Grant, C.** (1983) Nearshore fringing reefs in north Queensland. *Coral Reefs*, **1**, 151-160.

Hovland, M. (1990) Do carbonate reefs form due to fluid seepage? *Terra Nova*, **2**, 8-18.

Hovland, M. and **Judd, A.G.** (1988) *Seabed pockmarks and seepages. Impact on Geology, Biology and the Marine Environment.* Graham & Trotman, London, 293 pp.

Hovland, M., Mortensen, P.B., Brattegard, T., Strass, P. and **Rokoengen, K.** (1998) Ahermatypic coral banks off mid-Norway: evidence for a link with seepage of light hydrocarbons. *Palaios*, **13**, 189-200.

Hovland, M., Talbot, M.R., Qvale, H., Olaussen, S. and **Aasberg, L.** (1987) Methane-related carbonate cements in pockmarks of the North Sea. *J. Sed. Petrol.*, **57**, 881-892.

Hovland, M. and **Thomsen, E.** (1997) Cold-water corals- are they hydrocarbon seep related? *Mar. Geol.*, **137**, 159-164.

J**ensen, P., Aagaard, I., Burke, Jr.R.A., Dando, P.R., Jorgensen, N.O., Kuijpers, A., Laier, T., O'Hara, S.C.M.** and **Schmaljohann, R.** (1992) 'Bubbling reefs' in the Kattegat: submarine landscapes of carbonate-cemented rocks support a diverse ecosystem at methane seeps. *Mar. Ecol. Prog. Ser.*, **83**, 103-112.

Johnson, D.P. and **Risk, M.J.** (1987) Fringing reef growth on a terrigenous mud foundation, Fantome Island, central Great Barrier Reef, Australia. *Sedimentology*, **34**, 275-287.

Kauffman, E.G., Arthur, M.A., Howe, B. and **Scholle, P.A.** (1996) Widespread venting of methane-rich fluids in Late Cretaceous (Campanian) submarine springs (Tepee Buttes), Western Interior seaway, U.S.A.. *Geology*, **24**, 799-802.

Kelly, S.R.A., Blanc, E., Price, S.P. and **Whitham, A.G.** (2000) Early Cretaceous giant bivalves from seep-related limestone mounds, Wollaston Foreland, northeast Greenland. In: *The evolutionary biology of the Bivalvia* (Eds E.M. Harper, J.D. Taylor, and J.A. Crame), *Geol. Soc. London, Spec. Publ.*, **177**, 227-246.

Kennett, J.P., Cannariato, K.C., Hendy, I.L. and **Behl, R.J.** (2000) Carbon isotopic evidence for methane hydrate instability during Quaternary interstadials. *Science*, **288**, 128-133.

Kulm, L.D. and **Suess, E.** (1990) Relationship between carbonate deposits and fluid venting: Oregon accretionary prism. *J. Geophys. Res.*, **95**, 8899-8915.

Lacombe, O., Angelier, J., Chen, H.W., Deffontaines, B., Chu, H.T. and **Rocher, M.** (1997) Syndepositional tectonics and extension-compression relationships at the front of the Taiwan collision belt: a case study in the Pleistocene reefal limestones near Kaohsiung, SW Taiwan. *Tectonophysics*, **274**, 83-96.

Lacombe, O., Mouthereau, F., Deffontaines, B., Angelier, J., Chu, H.T. and **Lee, C.T.** (1999) Geometry and Quaternary kinematics of fold-and-thrust units of SW Taiwan. *Tectonics*, **18**, 1198-1223.

Lewis, K.B. and **Marshall, B.A.** (1996) Seep faunas and other indicators of methane-rich dewatering on New Zealand convergent margins. *New Zealand J. Geol. Geophys.*, **39**, 181-200.

Liljedahl, L. (1992) The Silurian *Ilionia prisca*, oldest known deep-burrowing suspension-feeding bivalve. *J. Paleontol.*, **66**, 206-210.

Longman, M.W. (1981) A process approach to recognizing facies of reef complexes. In: *European fossil reef models* (Ed, D. F. Toomey), *SEPM Spec. Publ.*, **30**, 9-40.

MacDonald, I.R., Reilly, J.F.II, , Guinasso, N.L., Jr., Brooks, J.M., Carney, R.S., Bryant, W.A. and **Bright, T.J.** (1990) Chemosynthetic mussels at a brine-filled pockmark in the northern Gulf of Mexica. *Science*, **248**, 1096-1099.

Maslin, M., Mikkelsen, N., Vilela, C. and **Haq, B.** (1998) Sea-level- and gas-hydrate-controlled catastrophic sediment failures of the Amazon Fan. *Geology*, **26**, 1107-1110.

McDonnell, S.L., Max, M.D., Cherkis, N.Z. and **Czarnecki, M.F.** (2000) Tectono-sedimentary controls on the likelihood of gas hydrate occurrence near Taiwan. *Mar. Petrol. Geol.*, **17**, 929-936.

Paull, C.K., Buelow, W.J., Ussler, W.III and **Borowski, W.S.** (1996) Increased continental-margin slumping frequency during sea-level lowstands above gas hydrate-bearing sediments. *Geology*, **24**, 143-146.

Paull, C.K., Chanton, J.P., Neumann, A.C., Coston, J.A., Martens, C.S. and **Showers, W.** (1992) Indicators of methane-derived carbonates and chemosynthetic organic carbon deposits: examples from the Florida Escarpment. *Palaios*, **7**, 361-375.

Peckmann, J., Thiel, V., Michaelis, W., Clari, P., Gaillard, C., Martire, L. and **Reitner, J.** (1999) Cold seep deposits of Beauvoisin (Oxfordian; southeastern France) and Marmorito (Miocene; northern Italy): microbially induced authigenic carbonates. *Intl. J. Earth Sci.*, **88**, 60-75.

Purser, B.H., Soliman, M. and **M'Rabet, A.** (1987) Carbonate, evaporite, siliciclastic transitions in Quaternary rift sediments of the northwestern Red Sea. *Sed. Geol.*, **53**, 247-267.

Reid, R.G.B. and **Brand, D.G.** (1986) Sulfide-oxidizing symbiosis in lucinaceans: implications for bivalve evolution. *Veliger*, **29**, 3-24.

Reilly, Jr.J.F., MacDonald, I.R., Biegert, E.K. and **Brooks, J.M.** (1996) Geological controls on the distribution of chemosynthetic communities in the Gulf of Mexico. In: *Hydrocarbon migration and its near-surface expression* (Eds D. Schumacher and M. A. Abrams), *AAPG Mem.*, **66**, 39-62.

Ritger, S., Carson, B. and **Suess, E.** (1987) Methane-derived authigenic carbonates formed by subduction-induced pore-water expulsion along the Oregon/Washington margin. *Geol. Soc. Am. Bull.*, **98**, 147-156.

Roberts, H.H. (1987) Modern carbonate-siliciclastic transitions: humid and arid tropical examples. *Sed. Geol.*, **50**, 25-65.

Roberts, H.H. (1992) Reefs, bioherms, and lithoferms of the northern Gulf of Mexico: the important role of hydrocarbon seeps. *Proc. 7th Intl. Coral Reef Symp., Guam*, **2**, 1121-1128.

Rogers, C.S. (1990) Responses of coral reefs and reef organisms to sedimentation. *Mar. Ecol. Prog. Ser.*, **62**, 185-202.

Sakai, H., Gamo, T., Ogawa, Y. and **Boulegue, J.** (1992) Stable isotopic ratios and origins of the carbonates associated with cold seepage at the eastern Nankai Trough. *Earth Planet. Sci. Lett.*, **109**, 391-404.

Scoffin, T.P. and **Le Tissier, M.D.A.** (1998) Late Holocene sea level and reef-flat progradation, Phuket, south Thailand. *Coral Reefs*, **17**, 273-276.

Strasser, A., Strohmenger, C., Davaud, E. and **Bach, A.** (1992) Sequential evolution and diagenesis of Pleistocene coral reefs (south Sinai, Egypt). *Sed. Geol.*, **78**, 59-79.

Suess, E., Torres, M.E., Bohrmann, G., Collier, R.W., Greinert, J., Linke, P., Rehder, G., Trehu, A., Wallmann, K., Winckler, G. and **Zuleger, E.** (1999) Gas hydrate destabilization: enhanced dewatering, benthic material turnover and larger methane plumes at the Cascadia convergent margin. *Earth Planet. Sci. Lett.*, **170**, 1-15.

Taberner, C. and **Bosence, D.W.J.** (1985) Ecological succession from corals to coralline algae in Eocene patch reefs, northern Spain. In: *Paleoalgology: contemporary research and applications* (Eds D. F. Toomey and M. H. Nitecki), pp. 226-236. Springer-Verlag, Berlin.

Taylor, J.D. and **Glover, E.A.** (2000) Functional anatomy, chemosymbiosis and evolution of the Lucinidae. In: *The evolutionary biology of the Bivalvia* (Eds E. M. Harper, J. D. Taylor and J. A. Crame), *Geol. Soc. London, Spec. Publ.*, **177**, 207-225.

Terzi, C. (1993) The <<Calcari a *Lucina*>> (*Lucina* Limestones) of the Tuscan-Romagna Apennines as indicators of Miocene cold seep activity (northern Apennines, Italy).

Giornale di Geologia, ser. 3[a], **55**, 71-81.

Tudhope, A.W. and **Scoffin, T.P.** (1994) Growth and structure of fringing reefs in a muddy environment, south Thailand. *J. Sed. Res.,* **A64**, 752-764.

Weiss, M.P., Goddard, D.A. and **Picard, X.** (1978) Marine geology of reefs and inner shelf, Chichiriviche, Estado Falcon, Venezuela. *Mar. Geol.*, **28**, 211-244.

Woodroffe, C.D., Kennedy, D.M., Hopley, D., Rasmussen, C.E. and **Smithers, S.G.** (2000) Holocene reef growth in Torres Strait. *Mar Geol*, **170**, 331-346.

Yeh, M.G. and **Chang, Y.L.** (1991) The ichnofacies study of the Ailiaochiao Formation – the Changchihkeng Formation, Chiahsien- Meinung area, Kaohsiung. *Petroleum Geol. Taiwan*, **26**, 151-181.

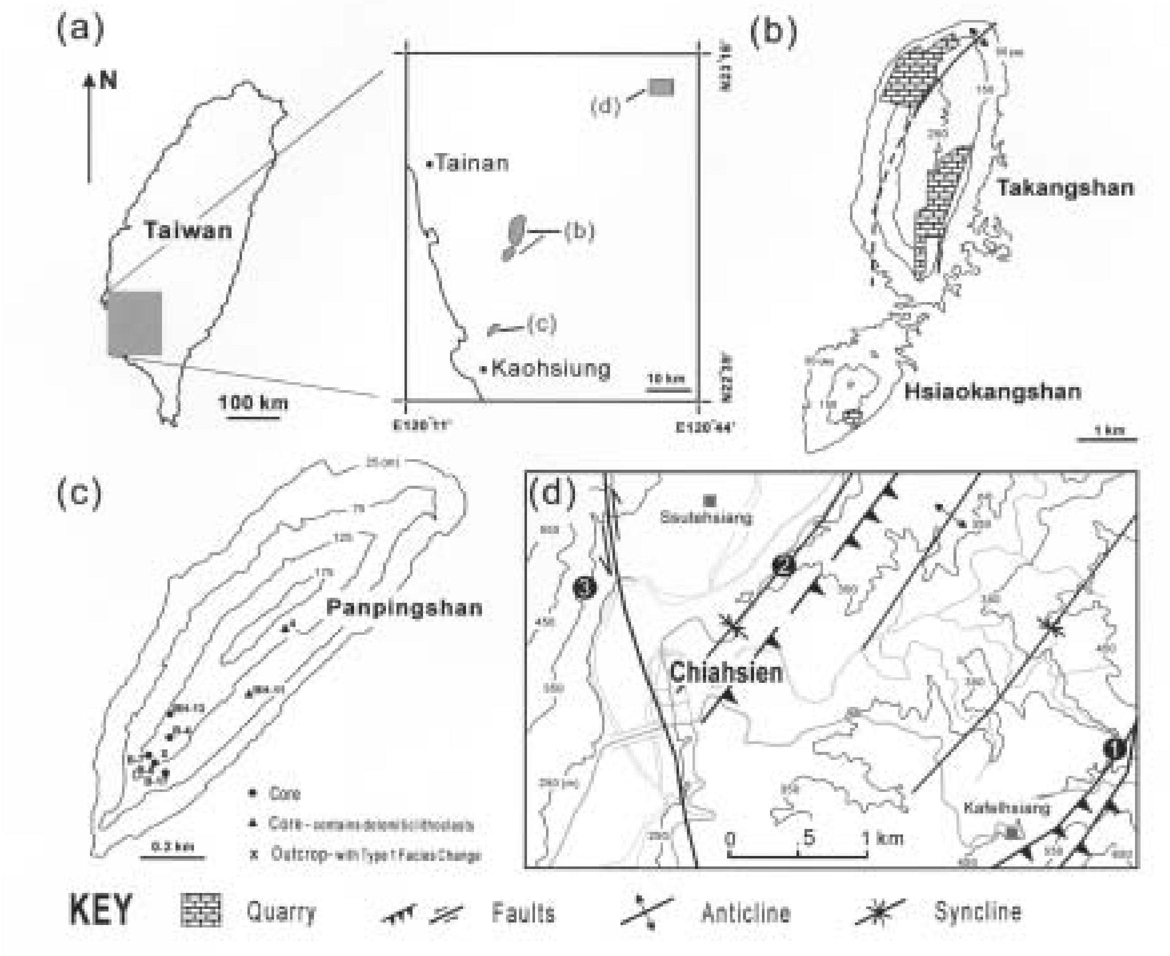

Fig. 1. (a) Outline map of Taiwan with the study area highlighted in grey. Letters in parentheses in the enlargement show the study localities in (b), (c) and (d). (b) Map showing the locations of quarries at Takangshan and Hsiaokangshan reefs. (c) Index map showing sites of borehole cores and observed outcrop in the Panpingshan quarry. (d) Map showing the study localities in Chiahsien Area; ❶:Paiyunhsiangku; ❷:Niupu; ❸:Ssutehsiang. Geological structures follow the geological map of the Chinese Petroleum Corporation (1989).

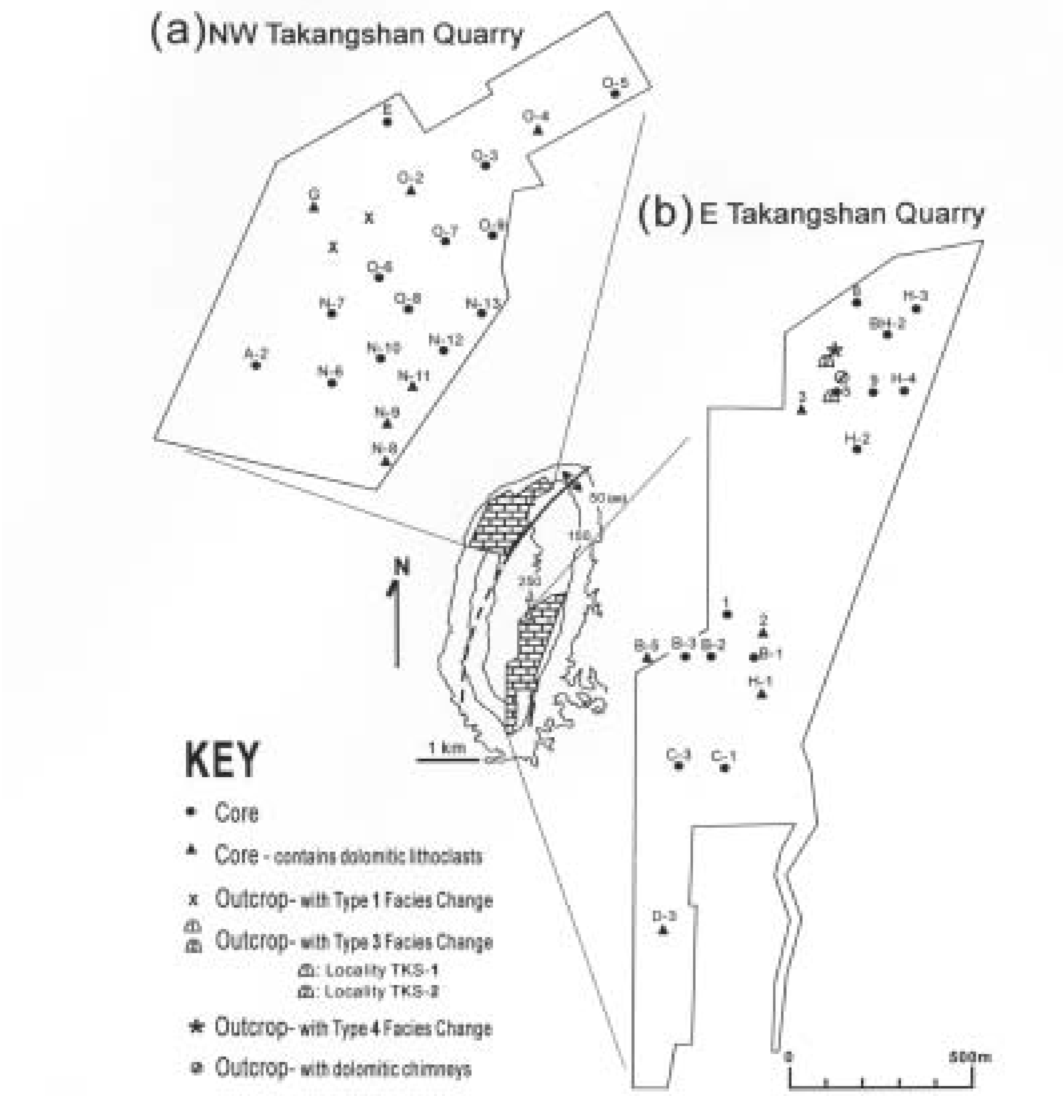

Fig. 2. Index maps showing sites of borehole cores and observed outcrops in the (a) NW and (b) E Takangshan quarries. The lithofacies associations observed at outcrops could be generalized as "mudstone- X- bioclastic limestone" in an ascending order. The "X" may be fossiliferous mudstone (Type 1 Facies Change), dolomitic mudstone (Type 3), muddy conglomerate (Type 4), or nothing (Type 2) at different locations. Scales for both index maps are the same.

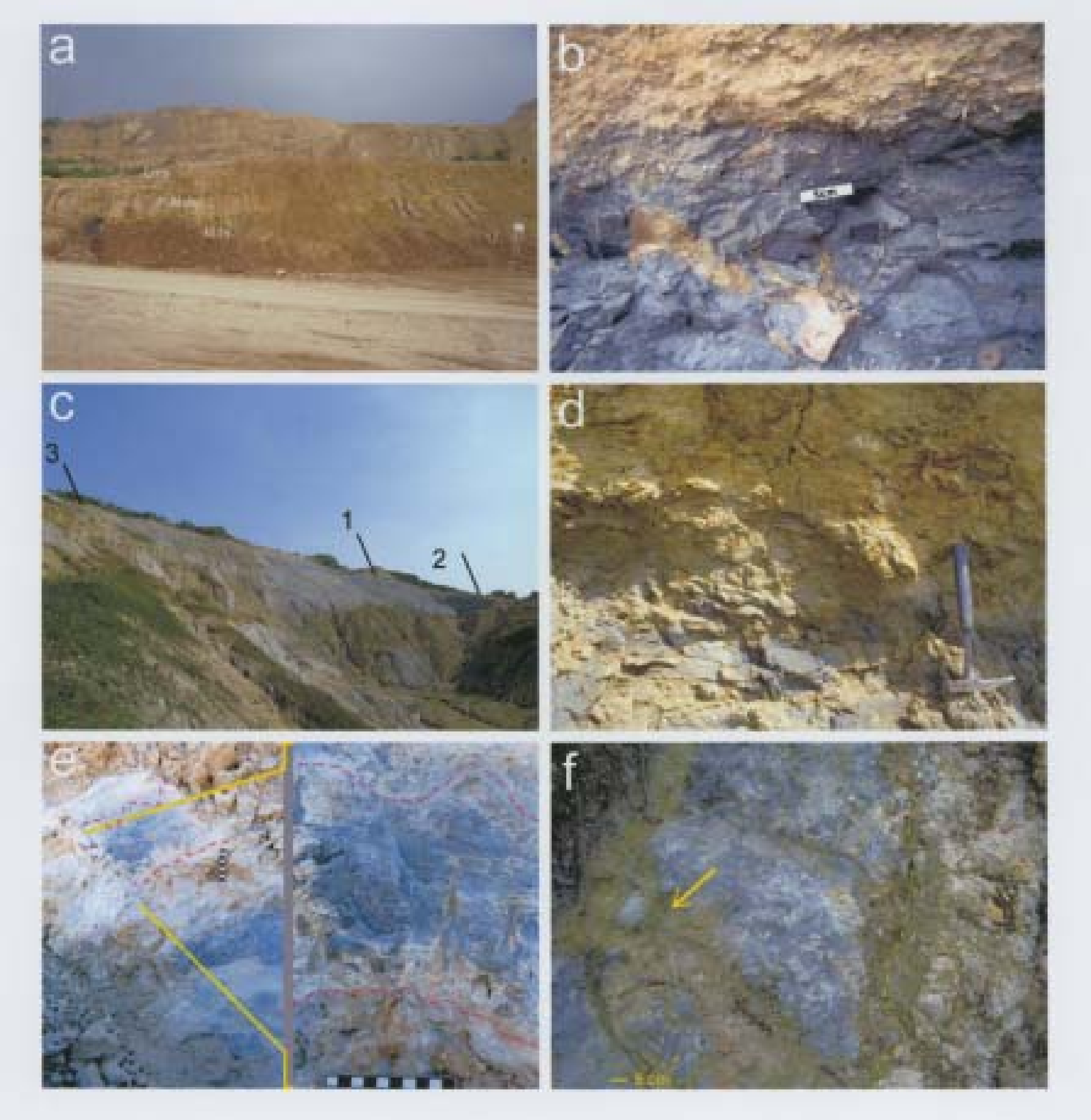

Fig. 3. (a) Outcrop with Type 1 Facies Change exposed at the NW Takangshan quarry. Both the top and bottom of fossiliferous mudstone are erosional surface. The thickness of the fossiliferous mudstone lithofacies at this location is about 60 cm. (b) Close-up of (a), showing rapid facies changes from the underlying mudstone upward into the fossiliferous mudstone. (c) Photograph showing the whole-view of quarry at E Hsiaokangshan; Site 1: outcrop with Type 2 Facies Change; Site 2: outcrop with dolomitic chimneys; Site 3: outcrop with lithified massive calcareous mudstones. (d) Close-up of Type 2 Facies Change at Site 1 in (c). (e) Outcrop of laminated coralline algae exposed at Locality TKS-1 of E Takangshan quarry. (f) Plane view showing an erosional surface at the top of dolomitic mound that was directly overlaid by bioclastic limestone at Locality TKS-2 in the E Takangshan quarry. The arrow marks an *in situ* fossil lucinid *L. golith* (Mds: mudstone; F-Mds: fossiliferous mudstone; Lms: bioclastic limestone).

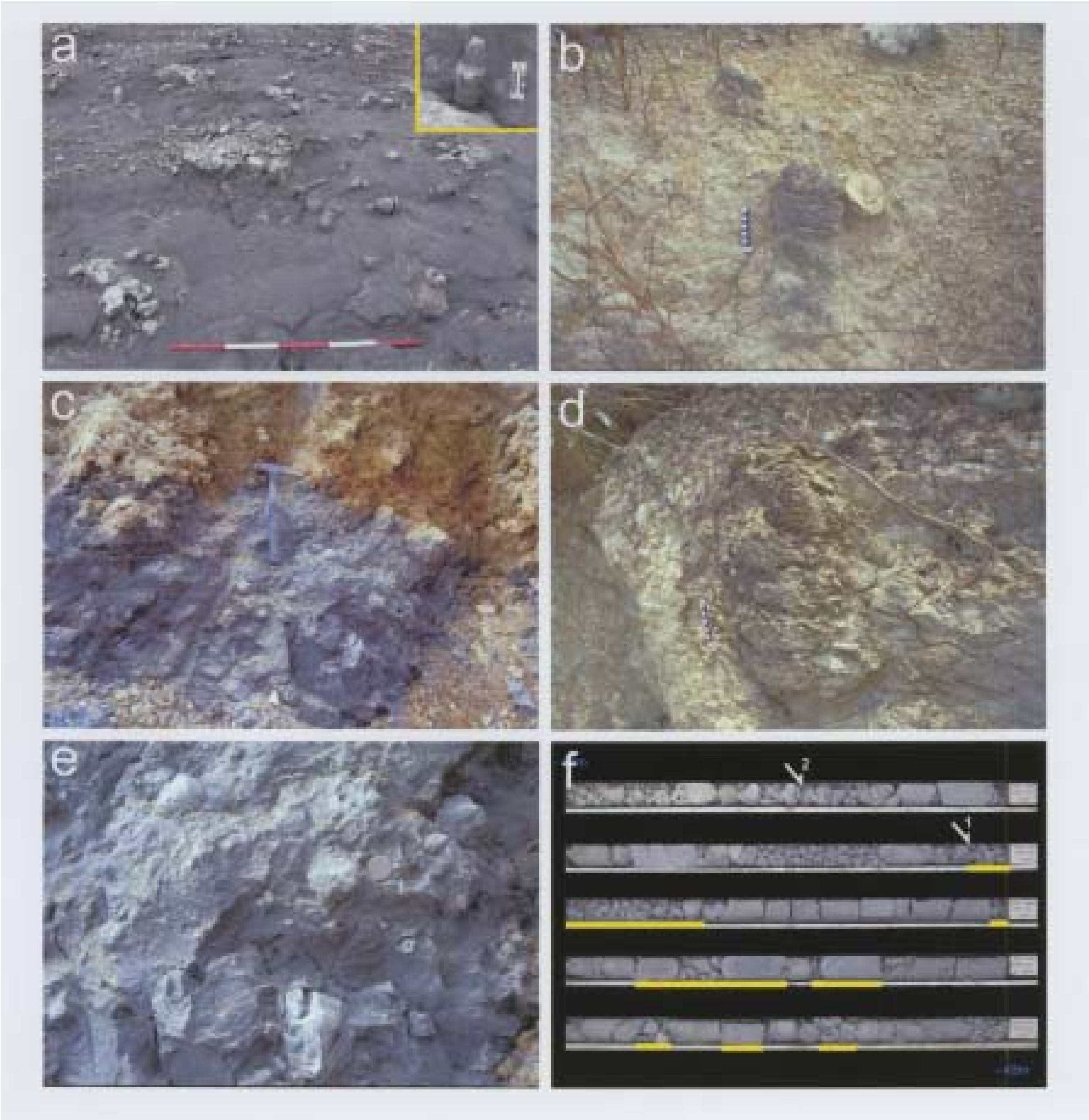

Fig. 4. (a) Plane view of massive mudstone with dolomitic chimneys exposed at the E Takangshan quarry. Inset on the upper right corner shows the close-up of a dolomitic chimney. (b) Photograph showing dolomitic chimneys protruding over the weathered topmost mudstones. Locality of this photography is situated at Site 2 in Fig. 3c. Scale is 10 cm long. (c) The Type 4 facies change outcropped at E Takangshan quarry. The top and bottom of muddy conglomerate (Congl.) are both erosional surfaces. (d) Side view of a mini plume-like dolomitic mudstone exposed at E Hsiaokangshan quarry. (e) Close-up of (c), showing well-lithified dolomitic lithoclasts occurred within the massive mudstones. (f) Borehole core no. 2 from the E Takangshan quarry showing the occurrences of dolomitic lithoclasts (underlined with yellow bars) within the mudstone lithofacies.

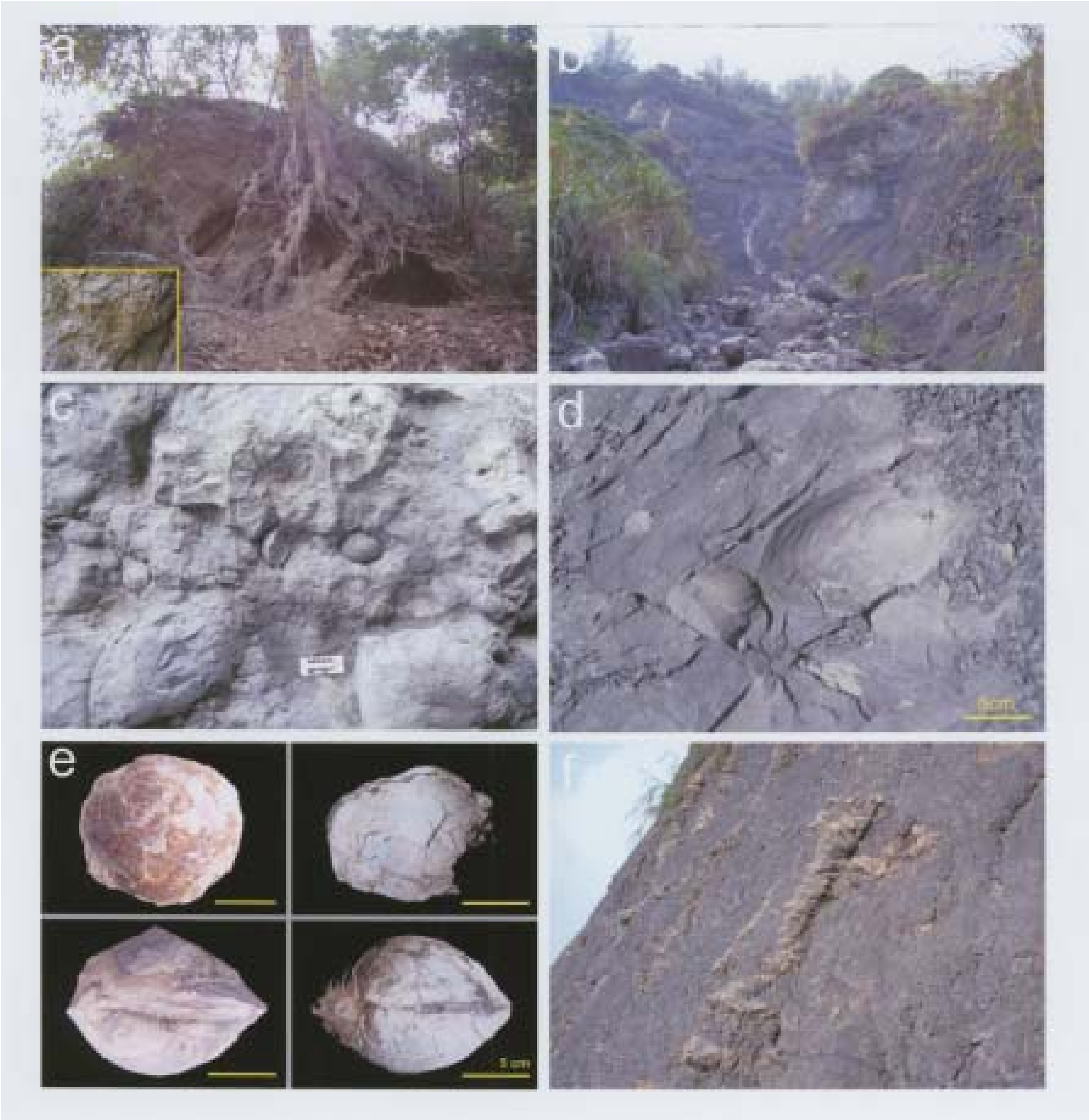

Fig. 5. (a) Mound-like dolomitic mudstone with a lateral extension of about 9.5 m outcropped at the Paiyunhsiangku in Chiahsien. Inset on the lower left corner shows abundant external shell molds of fossil lucinids in this lithology. (b) Photograph showing a giant dolomitic plume with a diameter of about 10 m outcropped at the Ssutehsiang in Chiahsien. A person stood aside this dolomitic plume for scale. (c) Photograph showing well preserved *in situ* fossil lucinids within the dolomitic plume outcropped at Ssutehsiang. (d) Photograph showing the crushed and/or flattened fossil lucinids occurred in the surrounding mudstones of dolomitic plume. (e) Fossil lucinids *L. goliath* collected from the dolomitic mudstones at Ssutehsiang (left two specimens) and E Takangshan quarry. The lengths of scale bars are the same. (f) Lateral view of dolomitic chimneys (*c.a.* 15-20 cm in diameters) at the Niupu outcrop in Chiahsien.

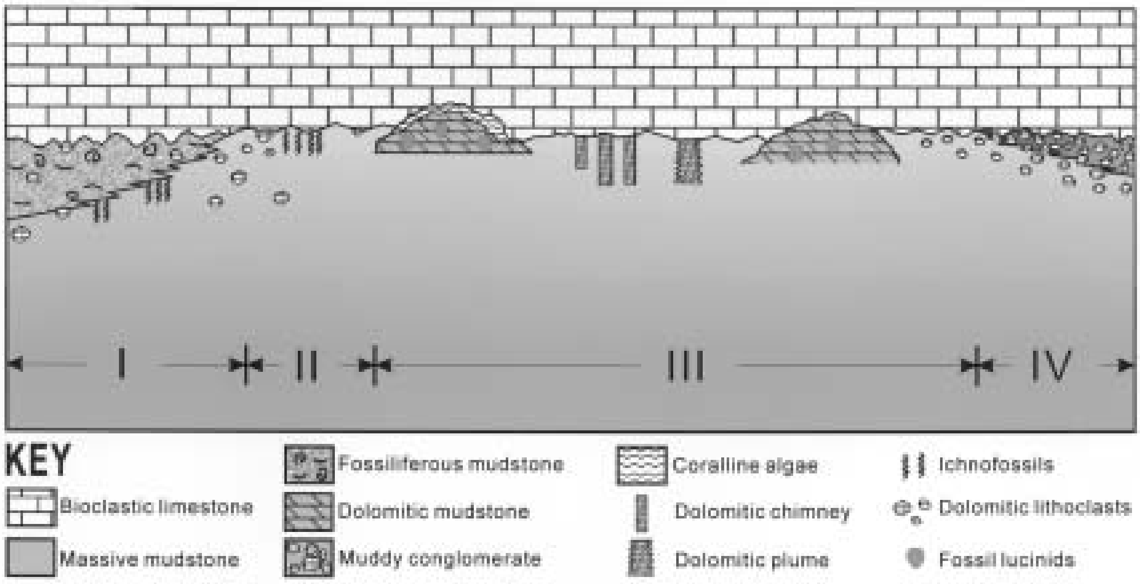

Fig. 6. Schematic draws illustrating various lithofacies changes from the underlying mudstone upward into the bioclastic limestone. Letters I, II, III, IV represent Type 1, 2, 3, and 4 facies associations observed within the study area, respectively. This synthetic picture is not to scale.